ANNALS of Clinical and Translational Neurology
Open Access
ANA American Neurological Association since 1875

RESEARCH ARTICLE

Susceptibility-weighted and diffusion kurtosis imaging to evaluate encephalomalacia with epilepsy after traumatic brain injury

Wenbin Li[1,2], Xuan Wang[1], Xiaoer Wei[1] & Mingliang Wang[1]

[1]Department of Radiology, Shanghai Jiao Tong University Affiliated Sixth People's Hospital, Shanghai 200233, China
[2]Imaging Center, Kashgar Prefecture Second People's Hospital, Kashgar, 844000 Xinjiang, China

Correspondence
Xuan Wang and Wenbin Li, Department of Radiology, Shanghai Jiao Tong University Affiliated Sixth People's Hospital, 600 Yishan Road, Shanghai 200233, China
Tel: 862124058993; Fax: 662164844183;
E-mails: 1072884137@qq.com;
liwenbin@sjtu.edu.cn

Funding Information
This study was funded by the National Natural Science Foundation of China (grant numbers: 81271540) and Natural Science Foundation of Xinjiang Province (grant number: 2016D01C083). Shanghai Key Discipline of Medical Imaging (grant number: 2017ZZ02005).

Received: 4 November 2017; Revised: 16 February 2018; Accepted: 17 February 2018

Annals of Clinical and Translational Neurology **2018; 5(5): 552–558**

doi: 10.1002/acn3.552

Wenbin Li and Xuan Wang are co-first authors.

Abstract

Objective: Encephalomalacia after traumatic brain injury (TBI) is one of the factors leading to epilepsy. In this study, magnetic resonance imaging (MRI) was used to explore the brain image features of epilepsy after traumatic encephalomalacia, and to provide objective evidence for predicting the possible occurrence of epilepsy after traumatic encephalomalacia. **Methods**: Two-hundred-fifty-two patients with traumatic encephalomalacia were prospectively enrolled in the study. All patients underwent MRI after discharge from the hospital. At the 1-year follow-up, participants were divided into epilepsy and nonepilepsy groups. All participants underwent MRI including conventional imaging, susceptibility-weighted imaging (SWI), and diffusion kurtosis imaging (DKI). The lesion volume, iron deposition, mean diffusion (MD), and mean kurtosis (MK) around the lesions were calculated for each group and compared using *t*-tests. P values < 0.05 were considered statistically significant. **Results**: Sixty patients with epilepsy and 91 without epilepsy were reported. There were no significant differences in Glasgow Coma Scale (GCS), lesion volume, encephalomalacia, or MD values between the two groups. Iron deposition was significantly higher in the epilepsy group ($P < 0.05$). The MK values were significantly different ($P < 0.05$). **Interpretation**: Advanced MRI is an important means of evaluating risk of developing epilepsy at 1 year due to encephalomalacia in patients with TBI. SWI and DKI could be used to assess the microstructural changes around the encephalomalacia, and therefore be used to evaluate risk of developing epilepsy at 1 year.

Introduction

Epilepsy is often observed in patients who have suffered brain trauma.[1–3] Determining the cause of and consequently predicting epileptic activity is of great clinical interest.[4] Brain tissue liquefaction necrosis or brain encephalomalacia are often caused by trauma, blood circulation disorders, infection, and other conditions.[3] Initially, microscopic manifestations of nerve cell death, interstitial edema, and inflammatory reactions occur,[2] followed by nerve cell loss,[5] and, consequently, encephalomalacia. Encephalomalacia alone likely does not cause epilepsy.[5] The cells around the region of encephalomalacia form lesions that appear as grayish white or grayish yellow fibrous scar tissue, with microscopic fiber bundles arranged in a crisscross pattern.[5,6] Proliferation of abnormal glial cells in the brain, fibrous scar tissue formation, and residual normal neurons[5] likely cause abnormal discharges and therefore epileptic activity.[7] Reactive glial cells play a role in repair and regulation in the brain.[8] However, too many glial cells are formed in the presence of a mechanical barrier, which hinders neuron growth, thereby causing a series of clinical symptoms that affect neuronal repair and functional recovery.[9,10]

Neuroimaging is considered to be an essential technique for determining the causes of epilepsy and location

and scope of the structures involved in the pathophysiology of epilepsy.[11–15] The onset of epilepsy often does not occur immediately after trauma,[11] and the interval between the occurrence of mild to moderate brain trauma and onset of epilepsy could range from 1 week to 2 years.[6,9,13] During this period, the main feature of the peripheral restoration of brain injury is encephalomalacia. In this study, we explored the use of recent MRI techniques to provide an objective basis for predicting the occurrence of posttraumatic epilepsy (PTE).[12]

Materials and Methods

Study Participants

A total of 252 patients (145 male, 107 female, average age 38.03 ± 13.31 years) with cerebral trauma were prospectively enrolled between Feb 2012 and Feb 2014. One year after discharge from the hospital, all patients underwent MRI, diffusion kurtosis imaging (DKI), and a susceptibility-weighted imaging (SWI) examination. All patients consented to the examination and signed an informed consent form. The study was approved by the ethics committee of Shanghai Jiao Tong University Affiliated Sixth People's Hospital.

Epilepsy diagnostic criteria

Our diagnostic criteria for epilepsy were based on the 1989 international league against epilepsy (ILAE) standards on epilepsy and classification.[16] Diagnosis of posttraumatic epilepsy (PTE) in patients with a history of trauma and epilepsy was made using the following diagnostic criteria: (1) no history of epilepsy prior to brain injury and hospital treatment; (2) no family history of epilepsy; (3) electrophysiological criteria for the spread of epilepsy, such as spike wave, spike and slow wave, sharp and slow wave, spike-slow wave, and focal high amplitude slow wave; (4) typical clinical manifestations of seizures, including loss of consciousness, senses, or movement; and (5) absence of other causes of epilepsy, including acquired and congenital diseases, such as cerebrovascular disease, infection, intracranial lesions, degenerative diseases, and brain abnormalities.

Inclusion criteria

A clear history of cerebral trauma; mild to moderate traumatic brain injury with a Glasgow Coma Scale (GCS) score of 9–15; follow-up period >1 year; absence of cerebral infarction, brain tumor, severe white matter damage, other neurological diseases, and serious chronic diseases; and encephalomalacia visible on conventional MR images were the inclusion criteria.

Grouping criteria

Grouping was performed by two doctors with >4 years work experience in neurosurgery, and they assigned GCS scores to patients as follows: mild traumatic brain injury: 13–15; moderate traumatic brain injury: 9–12.

Exclusion

Subjects who could not undergo MRI (such as subjects with magnetic pacemakers, in vivo magnetic metal foreign body, claustrophobia, etc.) were excluded. Patients who failed to complete the follow-up and MRI examination at 1 year were excluded.

MR examination and image processing

The scanner is a Siemens 3.0T (MAGENTOM, Verio, SiemensHealth-care, Germany) with 12 channel head surface coil. The conventional 3.0T MR imaging sequences used included T2-weighted imaging (T2WI), fluid attenuated inversion recovery (FLAIR), 3D-T1W, SWI, and DKI.

The SWI parameters were a TR/TE of 6000/95 msec, a base resolution of 384 × 384, a layer thickness of 6 mm, an interslice gap of 1.2 mm, and a matrix of 320 × 320.

The DKI parameters were 30 directions and 6*b* values (b = 0, 500, 1000, 1500, 2000, 2500 sec/mm^2), a voxel size of 2.3 × 2.3 × 4 mm^3, an FOV of 250 mm, a TR/TE of 1100/109 msec, and a layer thickness of 2 mm.

The volume of cerebral softening lesions was determined using the 3D-T1W sequence. Manual measurement of the volume of soft foci was mainly by a two-dimensional cross-sectional measurement of the single layer area, thickness, volume, and total volume of the unilateral hippocampus using the formula: V = (S1 + S2 + . . .Sn)× (layer thickness + layer spacing). V represents the absolute volume of the softening foci; S represents the area of the softening foci measured in each layer.

The area of bleeding foci detected by the SWI sequence was measured using Software Process Improvement Network (SPIN) software (process in neuroradiology SPIN, mrimaging.com website). The SWI map was opened in the SPIN software, and the approximate range of the lesion was drawn. The optimal threshold was then adjusted to completely cover the bleeding foci. The software then automatically calculated the coverage area—the pixel value of the bleeding area. This procedure was repeated for each region at the same level, and the total area of the bleeding foci was obtained.

ADC and DKI data were obtained using the different signal intensities, and the corresponding ADC diagrams and DKI diagrams were created by nonlinear fitting. Because the image background was uniform and the

foreground was clearly distinguished, we established a gray threshold before fitting so that the background was not included. We chose the Levenberg-Marquardt nonlinear fitting optimization method, and the size of the iteration step was given. The initial value was given to the fitting parameters for the MD and MK values in the actual fitting process for the iterative solution as follows: the program for the MD initial value (ln $S(0)$ J ln $S(b))/b)$, using an initial value in the range of 0.5–1.4. After fitting, a series of different MD values and MK values was obtained. Obviously, abnormal MD and MK values were caused by the interference of the final display. The MD and MK values shown are the MD and MK values from DKI.

Statistical analysis

Statistical tests were performed with the Statistical Package for Social Sciences software for Windows version 16.0. All of the quantitative variables are expressed as the mean (standard deviation). Group differences in the MRI parameter data were compared by two-sample *t*-tests. $P < 0.05$ indicated statistical significance.

Results

A total of 252 patients were selected according to the standard inclusion criteria. One-hundred-fifty-one patients with encephalomalacia (60 cases in the epilepsy group, 91 cases in the nonepilepsy group) were included in this study. The locations of encephalomalacia were observed, and there was no significant difference between the two groups in brain lobe distribution. The brain lobe encephalomalacia distribution characteristics of patients with and without epilepsy are shown in Table 1.

Comparisons of the encephalomalacia volume, DKI parameters and iron deposition in the epilepsy and nonepilepsy groups are shown in Table 2. There was no statistically significant difference in the volume of brain encephalomalacia lesions between the epilepsy and nonepilepsy groups, as shown in Table 2. The peripheral MK showed a statistically significant difference between the two groups, whereas the MD values did not. The SWI measurements showed statistically significant differences in the iron deposits around the peripheral area of encephalomalacia in patients with epilepsy compared to those in nonepileptic patients. Images of different patient scans are shown in Figure 1.

Table 1. Encephalomalacia sites in patients with epilepsy and without epilepsy after TBI.

	Epilepsy (+)	Epilepsy (−)	Total patients
Frontal lobe	15	25	45
Parietal lobe	11	15	26
Temporal lobe	20	28	53
Occipital lobe	10	16	26
More than one lobe[1]	4	7	11
Total	60	91	151

[1]Patients with encephalomalacia in more than one lobe.

Table 2. Comparison of the encephalomalacia volume, DKI parameters, and iron deposition in the epilepsy and nonepilepsy groups.

	Epilepsy group		Nonepileptic group		
	Mean	SD	Mean	SD	*P*-value
Volume (mm^3)	2.58	1.34	2.05	0.72	0.245
MK value	0.611	0.202	0.411	0.202	0.035
MD value	1.65	0. 471	1.732	0.573	0.291
SWI (ppm)	−5.461	2.053	−4.256	2.841	0.002

Discussion

Significance of multimodality MR imaging for the assessment of epilepsy

There have been several international reports on the correlation between the type of TBI and incidence of PTE.[1–5] A published report shows a PTE incidence rate of 5.0% during the first 3 years after trauma in 2826 TBI patients, with 66.0% occurring within the first 6 months after injury and 76.9% within the first 12 months after TBI.[17] The cumulative incidence rates of PTE for mild, medium, and severe injuries are 3.6%, 6.9%, and 17.0%, respectively, based on GCS classification.[17] The long-lasting high risk of epilepsy after brain injury might provide a window for the prevention of posttraumatic epilepsy. The risk of epilepsy is increased after a mild brain injury (relative risks 2.22, 95% 2.07–2.38) and a severe brain injury (7.40, 6.16–8.89). The risk is increased by more than 10 years after mild brain injury (1.51, 1.24–1.85) and severe brain injury (4.29, 2.04–9.00).[18] Emanuelson I identified PTE 10 years after TBI in a population-based, retrospective, follow-up study, and 12 of 109 participants developed active epilepsy during the follow-up period. The incidence of developing PTE within 10 years after a TBI was 11% in this series.[19] The incidence of PTE is directly related to the severity of the brain injury. GCS scores were used to select patients with mild to moderate TBI and to avoid inclusion of heavy injury patients. In our study, there was no significant difference between the GCS scores of the epilepsy and nonepilepsy groups, and patients with mild to moderate TBI complicated with softening foci showed a higher incidence of epilepsy, consistent with previous reports.[10,16,20] We speculate that for patients complicated with softening foci in this study, the possibility of a severe

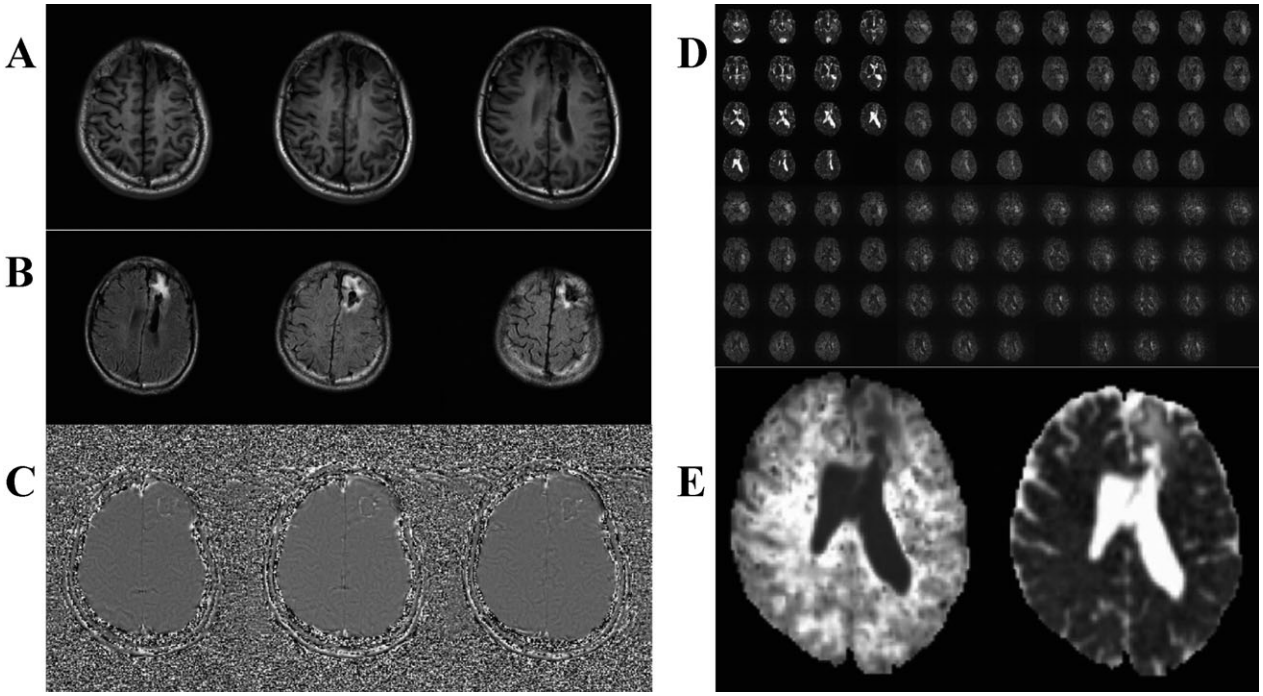

Figure 1. Images of the patient with each scan method. (A) T1W images of the patient. The left frontal lobe shows the shape of the lesion, and T1W had a low signal. (B) Representative flair images from a typical patient 1 year after traumatic brain injury. The left frontal lobe showed patch encephalomalacia around the glial proliferation zone. (C) SWI images of the patient. The left frontal lobe shows the shape of the lesion, which had high signal on the SWI phase map. (D) DKI images of the patient. The left frontal lobe shows the shape of the patch, which had a high signal on the DKI map. (E) MK and MD images of the patient. The left frontal lobe shows the shape of the patch, which had a low signal on MK and high signal on MD.

cerebral contusion and intracranial hematoma was increased, which increased the risk of PTE.[15]

The pathological basis of PTE is scar formation in the brain and glial proliferation.[5] Because of the shrinkage of scar tissue, brain tissue could be pulled toward the scar tissue, resulting in mechanical tension on the neurons, possibly causing epileptic foci.[2] FLAIR sequences can display lesions that are difficult to visualize using T2WI. Moreover, FLAIR is useful for studying the internal structure of lesions in the context of pathology. Therefore, FLAIR can be used as a routine examination method to reflect glial proliferation.[21] DKI is more sensitive to damage after TBI.[22] DKI mainly focuses on the intracellular and extracellular components of the nervous system; its structural characteristics are reflected by the degree of tissue diffusion, such as gray matter and white matter diffusion. In the case of random motion, the diffusion motion of water molecules satisfies the Gaussian distribution. For real biological tissue, the diffusion of water molecules occurs between the intercellular spaces and cells. This movement is not necessarily free movement, and therefore, the true movement of the water molecules is non-Gaussian in distribution. The greater the degree of water molecule diffusion in the surrounding environment, the more complex the constituent elements in the body and the more obvious the non-Gaussian dispersion. The initial goal of the DKI model was to quantify the extent of dispersion from the Gaussian distribution. The DKI model of organization of diffusion components was created without the assumption of benefits of model variables and stability calculations, so it reflects various microstructural changes. DKI provides a new perspective and thereby enhances clinical applications.

There were significant differences in the kurtosis values measured around the softening foci in the epileptic and nonepileptic groups. MK is considered to be a micro index complex and can be used to describe the structure of gray and white matter independent of spatial orientation. MK is used to determine the average value of the gradient direction with multiple b values and different directions. The value of MK depends on the complexity of the structure of the region of interest: the more complex the structure, the more significant the abnormal distribution of water molecules and larger the corresponding MK.[22] The diffusion of water molecules is restricted by many factors in living cells, and structures such as the cell membrane, axons, and myelin sheath (which are

approximately 5–30 μm) are theoretically able to block this diffusion.[23] Peripheral glial proliferation, neuronal degeneration, atrophy, and apoptosis lead to a decrease in the complexity of brain tissue and therefore a decrease in the MK value. In this study, softening of the foci around the glial hyperplasia likely led to an increase in MK values due to increased complexity in the epilepsy group. There was no significant difference between the two groups in terms of MD values. This finding could reflect the limited diffusion of water molecules in cells because the glial cell volume changes slowly in relation to the surrounding soft foci, unlike a brain edema caused by a cerebral infarction, which can be visualized within 15–30 min.

Iron and free radical damage after traumatic brain injury, extravasation of red blood cells, and dissolution and deposition of hemosiderin in the nerve fiber network are directly related to the occurrence of epilepsy.[20] Animal experiments confirmed that iron has a role in epilepsy, which is related to its redox properties.[24] Oxidation of iron leads to the formation of free radicals, causing cell membrane rupture, microenvironment changes, and ultimately, epilepsy.[24] SWI is an MRI sequence that uses a fully flow-compensated, long echo, gradient recalled echo (GRE) pulse sequence to acquire images. Magnitude and phase data are combined to produce an enhanced contrast magnitude image. This method exploits the susceptibility differences between tissues and uses the phase image to detect these differences. The SWI sequence is exquisitely sensitive to venous blood, hemorrhage, and iron storage.[25–27]

Prediction of epilepsy onset from softening around epileptic foci

In this study, changes in the microscopic structure of the brain related to PTE were explored using DKI and SWI, which mainly reflected changes in the structural complexity of the neurons and in iron deposits. DKI has been used in research on primary epilepsy.[22,28,29] In this study, the characteristics of epilepsy caused by soft foci were studied. Unlike most diseases studied by imaging, the PTE lesions cannot be accurately identified according to morphological abnormalities; most epileptic foci do not present with morphological abnormalities. In this study, the epileptic focus can be demonstrated by conventional MRI as a posttraumatic softening lesion of mixed gliosis.[30]

Astrocytes play an important role in the pathogenesis of epilepsy. In this study, evaluation of the MK value of DKI in brain tissue surrounding a softening focus could elucidate the pathological basis for proliferation and winding. In the FLAIR image, the ratio of myelomalacia surrounding a high signal intensity reached more than 85%. Glial repair after injury is likely the main process involved. Reactive astrogliosis is an important pathological characteristic of nervous system damage.

Most studies on epilepsy focus on induction by hemosiderin. Extravasation of red blood cells after TBI and dissolution and deposition of hemosiderin are significant features of trauma and are directly linked to epilepsy.[31] In this study, we used iron measurement methods, including a study of the high signal region and surrounding SWI, and a statistical comparison of the total pixel volume, ratio of the sum of the volume, and volume of the pixels. Based on our findings, we concluded the following. 1. The distribution of iron in the brain is not balanced. The iron contents in the basal ganglia and other parts of the gray matter as well as in the motor cortex are relatively high. Errors due to an irregular distribution could be reduced using the ratios of the regions of interest (ROIs).[32] 2. Because of the size of the hematoma, the shapes of the softening foci were irregular and the use of ratios of the form could reduce differences due to individual injuries.

The cumulative incidence of PTE in 30 years after mild, moderate, and severe TBI was about 2.1%, 4.2%, and 16.7%, respectively.[33] The follow-up time in this study was only 1 year. The incidence of epilepsy after TBI is not part of the study of more than 1 year, so the incidence of PTE may be underestimated. However, we do not know how many subjects will go on to develop epilepsy at time points beyond that. Let us speculate whether the MRI characteristics of our study evolve over time. After TBI, brain focal encephalomalacia lesions were formed,[5] and these changes could reduce the complexity of local brain tissue, leading to a decrease in the MK value.[34] Over time, glial hyperplasia was still the main pathological process surrounding the encephalomalacia.[35] Gliosis causes the complexity of regional structure to increase, and the MK value increases.[22] The relationship between the degree of gliosis and the degree of brain injury is not obvious. It is difficult to verify in histopathology. Therefore, as time goes on, this brings confusion to the interpretation of MK value.[32] With the extension of time, the unbalanced distribution of iron in the brain is quite different. Accuracy of SWI detection is affected.

A significant proportion of epilepsy occurs after mild and moderate brain trauma; but epilepsy usually did not occurred immediately after brain injury.[16] In fact, the occurring time of epilepsy varied after TBI. When are analyzed scans performed with respect to time of injury? Long-term dynamic studies, such as 1 year, 2 years, 5 years, 10 years, and 30 years of functional MRI tracking PTE, may be in a position to prevent bias. There would be a comprehensive understanding of PTE.

Conclusion

With the advent of new MRI techniques, the evaluation of mild to moderate posttraumatic encephalomalacia as an indicator of future epileptic activity is possible. SWI and DKI could be used to assess the microstructural changes around the encephalomalacia, and therefore be used to evaluate risk of developing epilepsy at 1 year.

Acknowledgments

This study was funded by the National Natural Science Foundation of China (grant numbers: 81271540) and Natural Science Foundation of Xinjiang Province (grant number: 2016D01C083). Shanghai Key Discipline of Medical Imaging (grant number: 2017ZZ02005).

Conflict of Interest

The authors declare that they have no conflict of interest.

References

1. Ranson D. Epilepsy and trauma. J Law Med 2003;10: 265–266.
2. Shorvon S, Neligan A. Risk of epilepsy after head trauma. Lancet 2009;373:1060–1061.
3. Sapina L, Vuletic V, Lojen G, et al. Head trauma and posttraumatic epilepsy in Slavonski Brod, East Croatia, 1988-2008. Coll Antropol 2014;38:1077–1079.
4. Willmore LJ, Lowenstein DH. Epilepsy and trauma: a persistent challenge. Neurology 2010;75:202–203.
5. Kazemi H, Hashemi-Fesharaki S, Razaghi S, et al. Intractable epilepsy and craniocerebral trauma: analysis of 163 patients with blunt and penetrating head injuries sustained in war. Injury 2012;43:2132–2135.
6. Benardo LS. Prevention of epilepsy after head trauma: do we need new drugs or a new approach? Epilepsia 2003;44 (Suppl 10):27–33.
7. Fleisher W, Staley D, Krawetz P, et al. Comparative study of trauma-related phenomena in subjects with pseudoseizures and subjects with epilepsy. Am J Psychiatry 2002;159:660–663.
8. Goncharuk OA, Il'kin AV. The treatment characteristics of epilepsy patients after craniocerebral trauma. Lik Sprava 1998;2:99–101.
9. Dudek FE. Is modulation of cortical synapses after brain trauma homeostatic? Or, since when is epilepsy normal? Epilepsy Curr 2009;9:53–54.
10. Melhem ER, Hoon AH Jr, Ferrucci JT Jr, et al. Periventricular leukomalacia: relationship between lateral ventricular volume on brain MR images and severity of cognitive and motor impairment. Radiology 2000;214: 199–204.
11. Gauffin H, Landtblom AM. Epilepsy and violence: case series concerning physical trauma in children of persons with epilepsy. Neuropsychiatr Dis Treat 2014;10: 2183–2189.
12. Wilson DA, Steiner RE. Periventricular leukomalacia: evaluation with MR imaging. Radiology 1986;160:507–511.
13. Baker LL, Stevenson DK, Enzmann DR. End-stage periventricular leukomalacia: MR evaluation. Radiology 1988;168:809–815.
14. Bozzao A, Di Paolo A, Mazzoleni C, et al. Diffusion-weighted MR imaging in the early diagnosis of periventricular leukomalacia. Eur Radiol 2003;13: 1571–1576.
15. Machilsen B, d'Agostino E, Maes F, et al. Linear normalization of MR brain images in pediatric patients with periventricular leukomalacia. NeuroImage 2007;35:686–697.
16. Breteler MM, de Groot RR, van Romunde LK, et al. Risk of dementia in patients with Parkinson's disease, epilepsy, and severe head trauma: a register-based follow-up study. Am J Epidemiol 1995;142:1300–1305.
17. Zhao Y, Wu H, Wang X, et al. Clinical epidemiology of posttraumatic epilepsy in a group of Chinese patients. Seizure 2012;21:322–326.
18. Christensen J, Pedersen MG, Pedersen CB, et al. Long-term risk of epilepsy after traumatic brain injury in children and young adults: a population-based cohort study. Lancet 2009;373:1105–1110.
19. Emanuelson I, Uvebrant P. Occurrence of epilepsy during the first 10 years after traumatic brain injury acquired in childhood up to the age of 18 years in the south western Swedish population-based series. Brain Inj 2009;23: 612–616.
20. Engel J Jr. ILAE classification of epilepsy syndromes. Epilepsy Res 2006;70(Suppl 1):S5–S10.
21. Fukuda K, Kirino T, Fujiwara Y, et al. Clinical aspects of epilepsy in children with periventricular leukomalacia. No To Hattatsu 2010;42:291–295.
22. Zhuo J, Xu S, Proctor JL, et al. Diffusion kurtosis as an in vivo imaging marker for reactive astrogliosis in traumatic brain injury. NeuroImage 2012;59:467–477.
23. Gao Y, Zhang Y, Wong CS, et al. Diffusion abnormalities in temporal lobes of children with temporal lobeepilepsy: a preliminary diffusional kurtosis imaging study and comparison with diffusion tensor imaging. NMR Biomed 2012;25:1369–1377.
24. Grinberg F, Ciobanu L, Farrher E, et al. Diffusion kurtosis imaging and log-normal distribution function imaging enhance the visualisation of lesions in animal stroke models. NMR Biomed 2012;25: 1295–1304.
25. Rauscher A, Sedlacik J, Barth M, et al. Magnetic susceptibility-weighted MR phase imaging of the human brain. Am J Neuroradiol 2005;26:736–742.

26. Haacke EM, Mittal S, Wu Z, et al. Susceptibility-weighted imaging: technical aspects and clinical applications, part 1. AJNR Am J Neuroradiol 2009;30:19–30.
27. Mittal S, Wu Z, Neelavalli J, et al. Susceptibility-weighted imaging: technical aspects and clinical applications, part 2. AJNR Am J Neuroradiol 2009;30:232–252.
28. Winston GP. The potential role of novel diffusion imaging techniques in the understanding and treatment of epilepsy. Quant Imaging Med Surg 2015;5:279–287.
29. Zhang Y, Yan X, Gao Y, et al. A preliminary study of epilepsy in children using diffusional kurtosis imaging. Clin Neuroradiol 2013;23:293–300.
30. Wu EX, Cheung MM. MR diffusion kurtosis imaging for neural tissue characterization. NMR Biomed 2010;23:836–848.
31. Kielbinski M, Gzielo-Jurek K, Soltys Z. Roles for Astrocytes in Epilepsy: insights from malformations of cortical development. Neuropathol Appl Neurobiol 2016;42:593–606.
32. Huang LC, Wu MN, Chen CH, et al. Susceptibility-weighted imaging in patient with consciousness disturbance after traffic accident. Am J Emerg Med 2013;31:e261–e263.
33. Annegers JF, Hauser WA, Coan SP, et al. A population-based study of seizures after traumatic brain injuries. N Engl J Med 1998;338:20–24.
34. Immonen R, Kharatishvili I, Gröhn O, et al. MRI biomarkers for post-traumatic epileptogenesis. J Neurotrauma 2013;30:1305–1309.
35. Filibian M, Frasca A, Maggioni D, et al. In vivo imaging of glia activation using 1H-magnetic resonance spectroscopy to detect putative biomarkers of tissue epileptogenicity. Epilepsia 2012;53:1907–1916.

